Desalination and Water Treatment
www.deswater.com
doi: 10.1080/19443994.2014.908148

54 (2015) 1204–1215
April

Taylor & Francis
Taylor & Francis Group

Granular laterite for batch and column studies of phosphate removal and its modification with iron for enhancing the adsorption property

Qi Zhou, Jianyong Liu, Guangren Qian, Jizhi Zhou*

School of Environmental and Chemical Engineering, Shanghai University, 99 Shangda Road, Shanghai 200444, P.R. China, Tel. +86 21 66137746; Fax: +86 21 66137761; email: jizhi.zhou@shu.edu.cn

Received 2 December 2013; Accepted 15 March 2014

ABSTRACT

An aluminum iron-rich laterite with granular shape was developed as a phosphate absorbent candidate. Batch tests showed that phosphate sorption on the granular laterite (GL) was fitted well with the Langmuir and Freundlich models. The kinetics was the pseudo-second-order reaction. The physical characterization suggests that the adsorption and precipitation are responsible for P removal. Moreover, the adsorption of phosphate was highly pH dependent as high P removal amount was observed in the acidic solution. The presence of concomitant anions inhibited phosphate adsorption onto GL in the descending order of extent $NO_3^- > SO_4^{2-} > Cl^-$. Column experiments were carried out under a constant bed depth at different influent concentrations, which demonstrated that the capacities of the exhaustion point decreased with the increase of the influent concentration. Based on the results above, GL doped with iron was prepared. According to the response surface methodology, a Box–Behnken design (BBD) was applied to give the optimized preparation conditions (quality percentage concentration of 43%, activation time of 2.13 h, and impregnation time of 0.5 h). The estimated phosphorus sorption capacity under the optimized conditions was 1.542 mg P/g, which was much higher than that using GL without modification.

Keywords: Phosphate removal; Granular laterite (GL); Column adsorption; Granular laterite doped with iron (GL-Fe); Response surface methodology (RSM)

1. Introduction

Water eutrophication is a serious environmental problem worldwide as it destroys ecosystem and makes water quality worse by damaging the ecological balance, threatening drinking water safety, shrinking fish culture, and hampering tourism [1,2]. The reduction of the phosphorus level in the water body is considered to be the most effective way to control water eutrophication. Various techniques have been used for phosphate removal, including chemical precipitation [3,4], biological treatment [5], ion exchange [6] adsorption [7,8], etc. Among them, adsorption is one of the most attractive approaches with the advantages of operation simplicity, low operation cost, and effective removal without yielding harmful byproducts.

In recent years, considerable attention has been paid on the development of cost-efficient sorbents

*Corresponding author.

Presented at the 6th International Conference on the "Challenges in Environmental Science and Engineering" (CESE-2013), 29 October–2 November 2013, Daegu, Korea

such as alum sludge [9], red mud [10,11], fly ash [12], and other waste materials [13,14]. These sorbents can effectively remove phosphorus from wastewaters by absorption and/or precipitation of chemically stable phosphorus phases, due to their high aluminum, iron, or calcium contents [15–18]. Thus, substrates with similar compositions may potentially serve to be phosphorus-removing absorbents.

Laterite is a rich Fe–Al-oxide clay mineral formed under high temperature and humidity conditions in subtropical zone, which widely distributes in the subtropical hilly region mostly between latitude 25–31° with a total area of 56.9 million hectares in China. Due to its high content of active constituents such as aluminum, iron, and calcium, laterite has been used to remove fluoride [19], arsenate [20], Cu^{2+}, Zn^{2+}, Ni^{2+}, Cd^{2+}, and Cr^{6+} [21–23] from aqueous solution, and in particular phosphate [24–27] in the seawater. Accordingly, it is suggested that laterite, with economical feasibility and geographical availability, should be a type of competitive adsorbent for phosphate removal. In addition, the laterite after P saturated adsorption can be recycled as cheap phosphate fertilizer for plant growth without further treatment.

However, directly using laterite for phosphate removal is not appropriate as collection of the natural laterite powder would be very difficult after treatment with wastewater. Thus, raw laterite powders are processed to granular shapes featuring good physical strength, high chemical stabilities, and environmental friendliness. Hence, the granular laterite (GL) is suitable to be used in column technique for the phosphate removal under continuous flow conditions. On the other hand, an ideal adsorbent should be characteristic of low cost and high sorption capacity which satisfies both economic efficiency and operational convenience. Therefore, it is necessary to improve the adsorption efficiency of GL by modulating its surface with porous structures and compositions.

Surfactants are often added to increase the porosity of GL which improves its removal capacity of contaminants by increasing GL surface area. Sodium carboxy methyl cellulose (CMC) which is water soluble, not only provides an effective binder for laterite particles, but also acts as the pore-forming agent through burning loss at high temperatures. Compared with the previous work for granulation [19,28], the above-mentioned method requires a simpler process and efficiently makes use of the active sites inside the adsorbent.

Finally, ferric oxides have proved to be an effective material for specific removal of anionic pollutants, namely, arsenite/arsenate [29], selenite [30], or phosphate [31,32]. This suggests that loading of Fe_2O_3 onto GL surfaces can enhance the P removal efficiency.

Herein, the objectives of this study are to: (i) prepare the GL, (ii) perform batch studies to examine phosphate adsorption using the GL, (iii) perform column studies to investigate the phosphate uptake capacity of the GL under different influent concentrations, and (iv) prepare the Granular laterite doped with iron (GL-Fe) composite and optimize the preparative conditions by response surface methodology (RSM).

2. Materials and methods

2.1. Materials

All the chemicals were reagent grade from Sinopharm Chemical Reagent Co., Ltd. (China) and used without further purification. Laterite is taken from a mountain in Dali Bai Autonomous Prefecture, Yunnan Province. Phosphate solution was prepared by dissolving potassium dihydrogen phosphate ($KH_2PO_4 \rightarrow K^+ + H_2PO_4^-$) in real tail water which was obtained from the sewage treatment plant with the phosphate concentration of 2.0 mg P/L.

2.2. Preparation and characterization of granular laterite (GL-Fe)

The raw laterite was used for granulation. Before the granulation procedure, the laterite was first dried at 105°C for 24 h, and then the dried laterite samples were crushed in a mortar and sieved through a 40 mesh sieve. Hence, GL was prepared according to the procedure described as follows: 30 g of pretreatment laterite, sodium CMC at a dosage (mg/g) were mixed until evenly homogenizing. Afterwards, some boiling water was added into the mixture until pasting, and then granulation was carried out by the squeezing granulator. The resulted granules were dried under environment temperature and moisture for 24 h. Finally, the dried granules were roasted and calcined at 450°C for 2 h. The surface morphology of the GL was observed with Leica stereoscan 420 scanning electron microscope (SEM) (Leica, Germany), and XRD-600 (Shimadzu Corporation, Japan) were used for chemical analysis.

2.3. Batch adsorption experiments of GL

The phosphate solution was prepared by dissolving an accurately weighed sample of potassium dihydrogen phosphate (KH_2PO_4, anhydrous) in deionized water to desired concentrations. The concentration of tail water of sewage treatment plant was 2.0 mg P/L.

Batch sorption experiments were performed in order to obtain factors for preparation and equilibrium data. Phosphate solution (40 mL) was introduced in Erlenmeyer flasks (100 mL), GL with 1.0–5.0 g/L dosage was added to the solution. The sealed flasks were then placed in a thermostatic shaker bath and shaken at 25˚C with 120 rpm. Each flask was removed after the required reaction time (36 h, as evidenced by the following kinetic studies), and the solution was filtered through a 0.45 μm syringe filter paper and analyzed for the adsorption efficiency. The solution pH was adjusted by HCl or NaOH solutions, and Na_2SO_4, NaCl or $NaNO_3$ solutions were added as sources of the competing anions when necessary, the adsorption process was performed under the condition of 2.0 mg P/L at the initial phosphate concentration, the 2.0 g/L dosage of adsorbent and the added competing anion concentration was 10.0 mg P/L.

As for the kinetic experiments, a fixed amount of adsorbent (0.4 g) was introduced to 200.0 mL of prepared phosphate solutions and real tail water (initial concentration: 2.0 mg P/L) in flasks. The flasks were shaken at 25˚C with 120 rpm. The equilibrium adsorption capacity was evaluated on the basis of a mass balance between the initial and final phosphate concentrations.

2.4. Column adsorption of GL

The column adsorption of GL was performed at the bed height of 55.0 cm by using a transparent organic glass packed column of 2.0 cm inner diameter and 60.0 cm high fitted with laterite (200.0 g). The feed liquid, containing different phosphate concentrations (1.0, 10.0, and 20.0 mg P/L), was passed through the column at the flow rate of 15.0 mL/min by peristaltic water pumps at 25˚C. The effluent liquid of 5.0 mL was sampled at predetermined time intervals to analyze the phosphate concentration until no further phosphate removal was observed. The breakthrough curve was examined by plotting the ratio of the C/C_0 (C and C_0 are the concentrations of phosphate in the effluent and the feed, respectively) against time.

In order to study the effect of the interfering ions on column adsorption of GL for phosphate, the feed phosphate solution (2.0 mg P/L) amended by different interfering ions (Cl^-, NO_3^-, and SO_4^{2-}) with the concentration of 5.0 mg P/L was pumped through at the flow rate of 15.0 mL/min.

2.5. Preparation of GL-Fe

The GL-Fe was prepared by impregnation method. Typically, the GL was soaked in ferric chloride solution (solid/solution ratio of 1/10 (w/w)). The amount $FeCl_3$ dissolved in the solution was 23–43% (w/w) of the GL dosage. The suspension was stirred for various times (0.5–2.5 h). After filtration through a 0.45 μm syringe filter paper, the modified GL was dried overnight at 105˚C and then placed in a crucible, calcined at 230˚C (the transformation temperature of ferric chloride change into iron oxide) in an oven for various time. The resultant GL-Fe was then collected and stored in the sealed glass vessel.

2.6. RSM experimental design and evaluation of the modified GL

RSM coupled with Box–Behnken experimental design (BBD) was applied to optimize the GL-Fe preparation conditions. The software of Design-Expert 7.1.6 was used for designing and analyzing the experimental data. The validity of the model was expressed in terms of the coefficient of determination R^2, and the adequacy of the model was further evaluated by analysis of variance (ANOVA). For statistical calculations, the variables X_i were coded as x_i according to Eq. (1):

$$x_i = \frac{X_i - X_0}{\delta X} \tag{1}$$

where X_i is the real value of the independent variable, X_0 is the real value of the independent variable at the center point, and δX represents the step change.

The quadratic equation model for predicting the objective function can be expressed according to Eq. (2), in which Y is the predicted response (phosphate removal), b_0 the constant coefficient, b_i the linear coefficients, b_{ii} the quadratic coefficients, b_{ij} the interaction coefficients, and x_i, x_j are the coded levels of process factors studied.

$$Y = b_0 + \sum_{i=1}^{k} b_i x_i + \sum_{i=1}^{k} b_{ii} x_i^2 + \sum_{i=1}^{k} \sum_{j=i+1}^{k} b_{ij} x_i x_j \tag{2}$$

2.7. Analytical methods

The concentrations of the phosphate solutions were determined by the ascorbic acid method [22], measuring the absorbance at 700 nm with the UV–vis spectrophotometer (Model 721, Shanghai Metash Instruments Co., Ltd, China). The pH of the solution was determined by Sartorius PB 220 pH meter (Sartorius, Germany).

The adsorption capability (Q_e, mg/g) of phosphate in adsorbent was calculated by the following equation:

$$Q_e = \frac{(C_0 - C_e)V}{m} \tag{3}$$

where C_0 and C_e (mg/L) are the initial and equilibrium liquid phase phosphate concentrations, respectively; V (L) is the volume of the solution and m (g) is the mass of the adsorbent.

The isotherm data were analyzed by Langmuir (Eq. (4)) and Freundlich (Eq. (5)) equations that can be expressed mathematically as follows:

$$\frac{C_e}{q_e} = \frac{C_e}{Q_{\max}} + \frac{1}{K_L q_{\max}} \tag{4}$$

$$\log q_e = \log K_f + \frac{\log C_e}{n} \tag{5}$$

where C_e is the equilibrium concentration of phosphate in solution (mg/L); q_e is the correspondent uptake capacity of the adsorbent (mg/g); $q_{\max}$ is the theoretical maximum phosphate adsorption capacity (mg/g), and K_L is the affinity constant (L/mg); and K_f (mg/g) and n are Freundlich constants.

To evaluate the adsorption kinetic process, the phosphate adsorption kinetic data is fitted by pseudo-first-order and second-order models. The kinetic equations for these models are as follows [33],

$$\log (q_e - q_t) = \log q_e - \frac{k_1 t}{2.303} \tag{6}$$

$$\frac{t}{q_t} = \frac{1}{k_2 q_e^2} + \frac{t}{q_e} \tag{7}$$

where q_e (mg/g) is the equilibrium adsorption capacity, q_t (mg/g) is the adsorption capacity of a moment (t); k_1 (min^{-1}) is the pseudo-first-order reaction kinetics constant; and k_2 (mg/g min) is quasi-second-order kinetic constants.

3. Results and discussion

3.1. The effect of surfactant dosage (mg/g) on P removal

Fig. 1 illustrates the phosphate (P) removal on 5.0 g/L of GL that was prepared by various amount of CMC added, where the initial concentration of phosphate was 20.0 mg P/L. The phosphate removal efficiency was increased with the CMC dosage increasing to 10 mg/g while decreased with CMC dosage increasing from 20 to 100 mg/g. The maximum P removal amount was obtained at the CMC dosage ranging from 10 to 20 mg/g. This indicates that at lower CMC dosage (<10 mg/g), the increase of P removal amount is contributed to the improvement of the specific surface area on GL as the formation of porous structure on GL by CMC addition. In comparison, the increase of CMC dosage (>20 mg/g) inhibited the P removal. This is mainly due to the fact that an excess of CMC was not completely removed at a high temperature, which resulted in the pore structure blocked by residual CMC. Accordingly, the adsorption of phosphate on GL was limited that decreased P removal amount, compared to that at low CMC dosage. Therefore, the 20 mg/g of CMC dosage was selected and the GL was press-casted as a cylindrical with 3 × 12 mm in size (inset) for the further experiment.

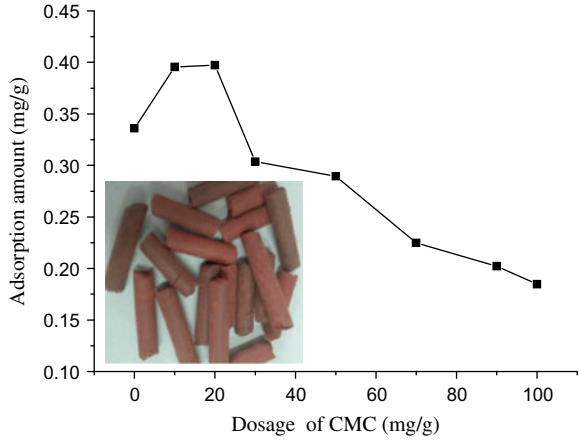

Fig. 1. Effect of different *dosage* (mg/g) of CMC on GL adsorption capacity (inset: prepared GL).

3.2. Characterization of GL

Fig. 2(a1) and (a2) shows the SEM images of GL surface before and after calcination, respectively. Compared to that before calcination, the dark shadows (arrows) in Fig. 2(a2) was observed in GL after calcination. This is probably contributed to the decomposition of CMC, which resulted in the rough surface on GL and the increasing of its surface area. This is beneficial for P adsorption performance, consistent with the improvement of P removal amount in Fig. 1.

Fig. 2 also exhibits the XRD pattern of GL before and after P removal. The phases of $K(Si_2Al)O_8$, Fe_2O_3, SiO_2 was identified on initial GL (Fig. 2(b1)), which indicates that GL was a fine-grained mixture of oxides and hydroxides. The Fe and Al content in GL was 19% as Fe_2O_3 and 44% as Al_2O_3, respectively. After

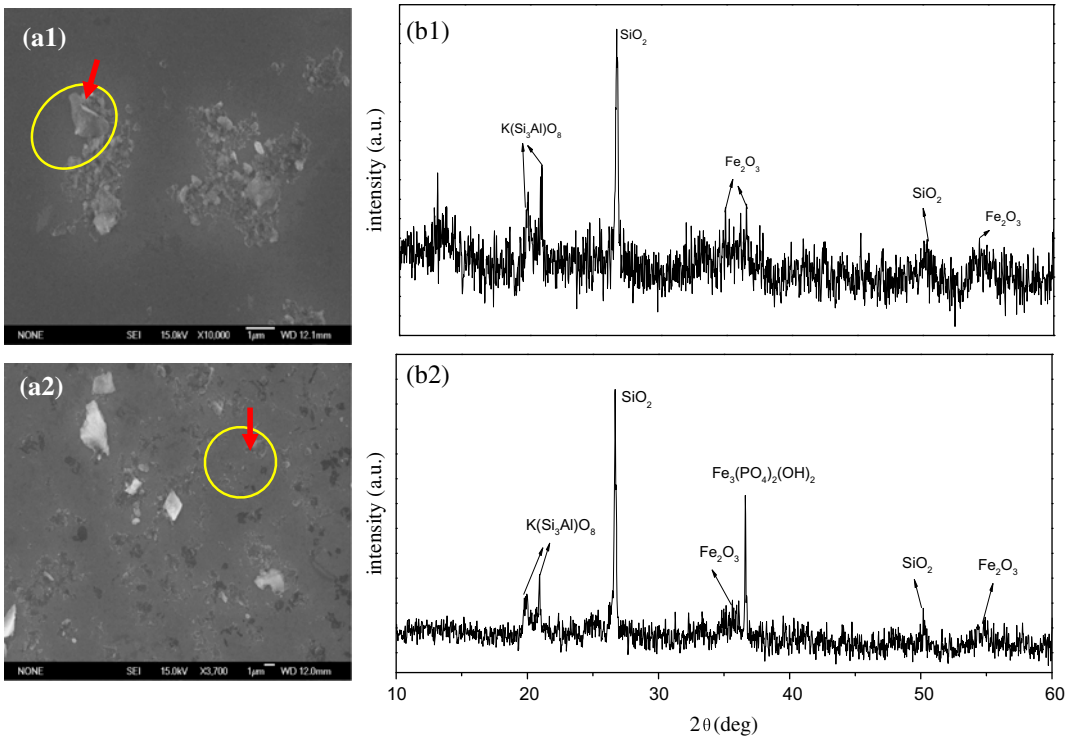

Fig. 2. The SEM of (a1) before roasting of GL and (a2) after *calcination* of GL; XRD pattern of (b1) GL and (b2) GL after adsorption.

removal, new phase of $Fe_3(PO_4)_2OH_2$ was observed (Fig. 2(b2)). Despite, the low signal-to-noise ratio suggests that the amount of new phase was low. This demonstrates that phosphate was predominantly removed by adsorption and precipitate in combination.

3.3. Batch adsorption experiments of GL

3.3.1. Uptake process of P

Fig. 3(a) shows the phosphate removal isotherm by varying the initial concentration of phosphate (0.5–15.0 mg P/L) with the dosage of 5.0 g/L. The P removal amount (q_e) increased with P equilibrium concentrations increasing. Fig. 3(b) and (c) illustrates that this P removal process was fitted by two typical isotherm models: Langmuir and Freundlich isotherms. Table 1 lists the fitting parameters, where the correlation coefficient R^2 for the corresponding model was 0.955 and 0.946, respectively. This indicates that the P uptake was well fitted by both models. Accordingly, the maximum P uptake capacity of the solid was estimated. For instance, the P uptake capacity of GL in the Langmuir model was 0.572 mg/g, which was higher than that of the limestone (0.25–0.3 mg P/g), dolomite and sand (0.052–0.168 mg P/g), and Peat (0.081 mg P/g) [34–37].

Fig. 4(a) exhibits the kinetics of P adsorption with P initial concentration of 2.0 mg P/L and GL dosage of 2.0 g/L. The removal of phosphate in the prepared phosphate solution increased with the increase of contact time. Fig. 4(b) and (c) shows the P uptake process fitted by the pseudo-first-order and pseudo-second-order plots. The resultant parameters were listed in Table 2, where the correlation coefficient was 0.999 in second-order model, higher than that in pseudo-first-order model. Moreover, the uptake of P in real tail water was performed on GL. As shown in Fig. 4, the similar process of P removal was observed, compared to that in the case of prepared solution. The pseudo-second-order model described well fitted the P uptake (Table 2). Therefore, it is proposed that the GL was a promising adsorbent for P removal in wastewater water.

3.3.2. Effect of initial pH and co-existing anions

As discussed above, the P removal on GL was a chemical adsorption process. Typically, this process is mainly affected by pH and co-existing anions. Fig. 5(a)

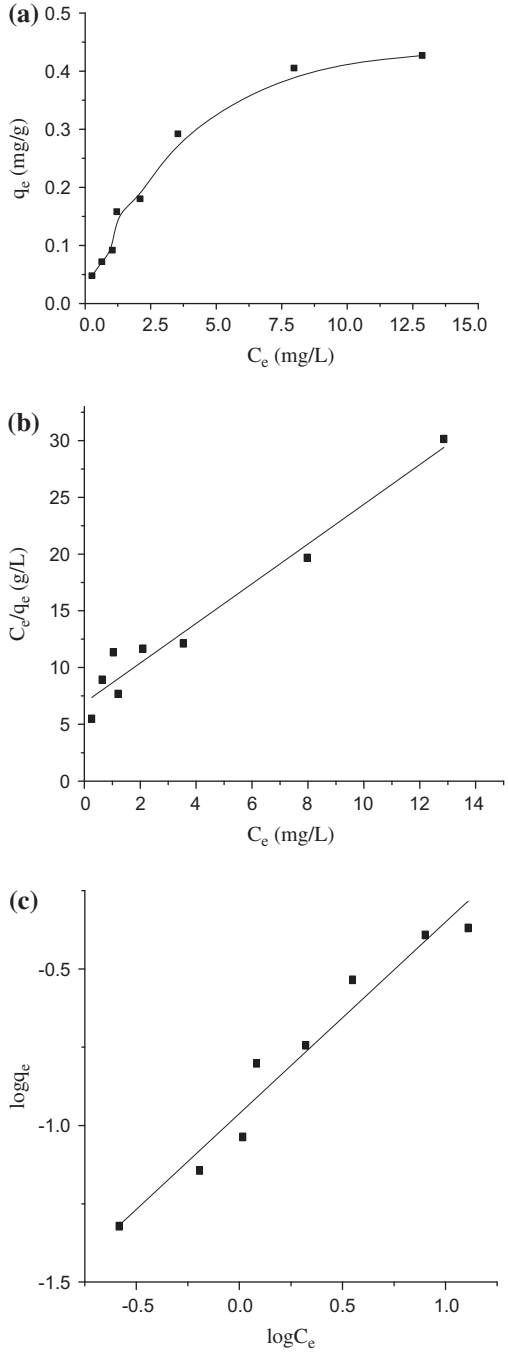

Fig. 3. (a) Isotherm of phosphate on GL, (b) linear Langmuir adsorption isotherm, and (c) Freundlich adsorption isotherm.

illustrates the P removal as a function of initial pH. The P removal amount was gently decreased by pH increasing to 6.0, followed by a sharp drop of P removal amount with pH increasing to 13.0. This is contributed to the changing of surface charge on GL. The pH at zero surface charge of GL was 7.3 [38], which means the positive charge on GL at pH < 7.3 while negative charge at pH > 7.3. As a result, a stronger affinity of phosphate anion with GL surface is proposed in acidic solution than that in basic solution. Accordingly, the P removal amount was reduced remarkably when initial pH increased. Moreover, the limited P removal in the basic solution was probably due to the competition between OH^- and phosphate on GL surface as well. For instance, there was 1.0×10^{-1} mmol/L of OH^- at pH = 10.0, higher than about 6.0×10^{-2} mmol/L of P (2.0 mg/L). This indicates that the surface charge and OH^- had effect on the P removal, which is in a good agreement with the results elsewhere [14,39].

Table 1
Langmuir and Freundlich isotherm parameters for phosphate adsorption

Langmuir			Freundlich		
Q_0 (mg/g)	K_L (L/mg)	R^2	n	K_f (mg/g)	R^2
0.572	0.254	0.955	1.635	0.109	0.946

Apart from OH^-, other co-existing anions also affect the P removal. As shown in Fig. 5(b), the decrease of P removal amount was observed in the presence of Cl^-, SO_4^{3-}, and NO_3^-, respectively. This indicates the competition between these co-existing anions and phosphate on GL surface. Moreover, the reduction amount of P was varied, which was dependent on the anions. Compared to that of 0.38 mg/g without co-existing anion, the adsorption amount of the phosphate was decreased to 0.25 mg/g in the presence of NO_3^-. This value was higher than that in the cases of Cl^- and SO_4^{3-}. Accordingly, the inhibition effect of anions on phosphate adsorption followed the order: $NO_3^- > SO_4^{2-} > Cl^-$. This is probably due to the smaller ion radius of NO_3^- than that of SO_4^{2-}, consistent with the results in the adsorption of phosphate elsewhere [40,41].

3.4. The column adsorption of GL

Fig. 6 illustrates the column test of phosphate removal on GL as a function of time, where the efficiency of phosphate removal was represented by the percentage of P concentration in effluence to the initial P concentration (C/C_0). As shown in Fig. 6(a), C/C_0 in all cases was increased to near 100%, and then kept constant with further increasing time. This indicates that the adsorption of P on GL was saturated after the increase of adsorption time in the column test. Moreover, this saturated time of P adsorption depended on

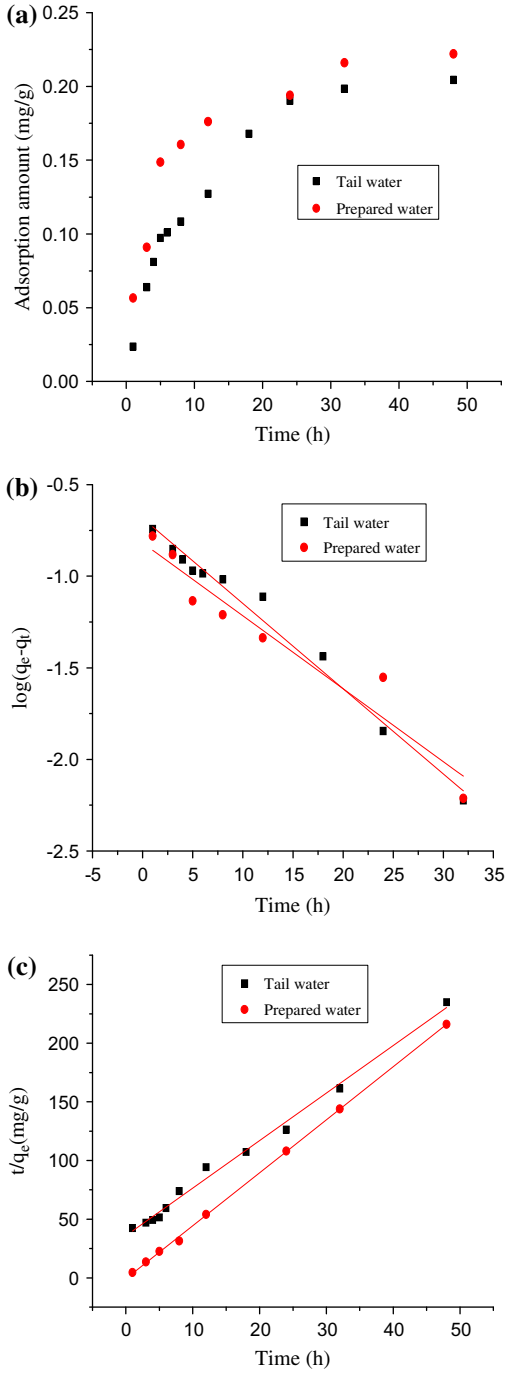

Fig. 4. (a) The rate of phosphate adsorption onto the sorbent GL under different circumstance, (b) pseudo-first-order model and (c) Pseudo-second-order model.

various initial phosphate concentration ([P]). For instance, near 100% of C/C_0 occurred in 1.5 h at initial [P] of 20 mg/g while in 7 h at initial [P] of 1 mg/g. This is attributed to the fact that the driving force of phosphate ions toward the binding sites (owing to concentration gradient phenomenon) was enhanced at high phosphate concentration, which led to high adsorption rate to make the active sites saturated more quickly in the column. In addition, the saturated time was also due to the fixed bed column with a low adsorbent filling quantity, which could not supply adequate contact time to maintain P concentration in the effluence at a low level.

Fig. 6(b) shows the practical kinetics of P removal in a real tail water of sewage treatment plant, where the influent concentration of P was 2.0 mg/L for the column test. Compared to that in the case of prepared solution (Fig. 6(a)), the P process in tail water was similar. The C/C_0 was 98% in 3 h then kept constant. Compared to that of 5 h in the case of prepared solution, the saturated time of P removal in real wastewater was shorter. This is likely related to the impurity in the real wastewater such as a large number of micro-organisms, suspended solids, algae, etc. These impurities had competitive adsorption toward the active sites, or were easy to adhere to the adsorbent surface to cause channel congestion, which resulted in the limited adsorption of phosphorus [42,43].

Fig. 7 shows the effects of Cl^-, NO_3^-, and SO_4^{2-} on the phosphate removal in the column test. Compared to that without co-existing anions, the increase of C/C_0 was more quickly in the presence of anions as the saturated time of P adsorption was 2–3 h in the cases of NO_3^-, and SO_4^{2-} and 4 h in the case of Cl^-. This demonstrates that the P adsorption in the column was inhibited by co-existing anions. Similar to that in the case of batch experiment, the inhabitation of P removal by anions is contributed to the competitive adsorption toward the active sites between phosphate ions and interfering ions.

3.5. Optimization of the GL-Fe modification

3.5.1. The effect of different variables on GL-Fe performance

As discussed above, the Fe content in GL has effect on the P removal. As a result, the modification of GL by $FeCl_3$ was carried out. Fig. 8 shows the performance of the resultant GL-Fe adsorbent (0.1 g/L) in P removal (initial [P] = 5.0 mg/L) with various modification conditions. As illustrated in Fig. 8(a), the phosphate uptake amount was increased from 0.93 to about 1.44 mg/g with the increase of the percentage of $FeCl_3$ to 38% in the solution. There was about 5% of Fe retained in the $FeCl_3$ solution after impregnation (not shown). This indicates that the improvement of P removal depended on the Fe loaded on GL. In comparison, with $FeCl_3$ at the percentage of 38 and 43%,

Table 2
Kinetic parameters for phosphate adsorption onto GL

Source of water body	Pseudo-first-order kinetics			Pseudo-second-order kinetics		
	k_1 (min^{-1})	q_e (mg/g)	R^2	k_2 (g/(mg h))	q_e (mg/g)	R^2
Prepared water	0.092	0.152	0.919	−22.8	0.221	0.999
Tail water	0.107	0.207	0.981	0.458	0.247	0.992

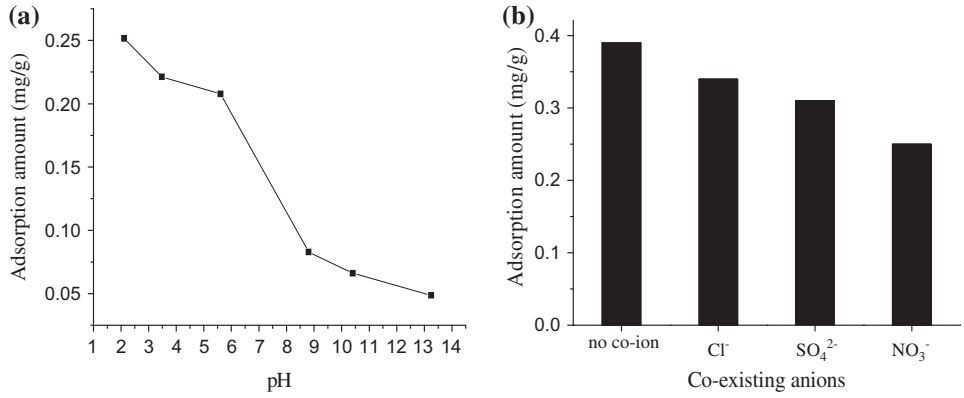

Fig. 5. Effect of (a) initial pH and (b) NO_3^-, SO_4^{2-}, Cl^- on phosphate adsorption in GL.

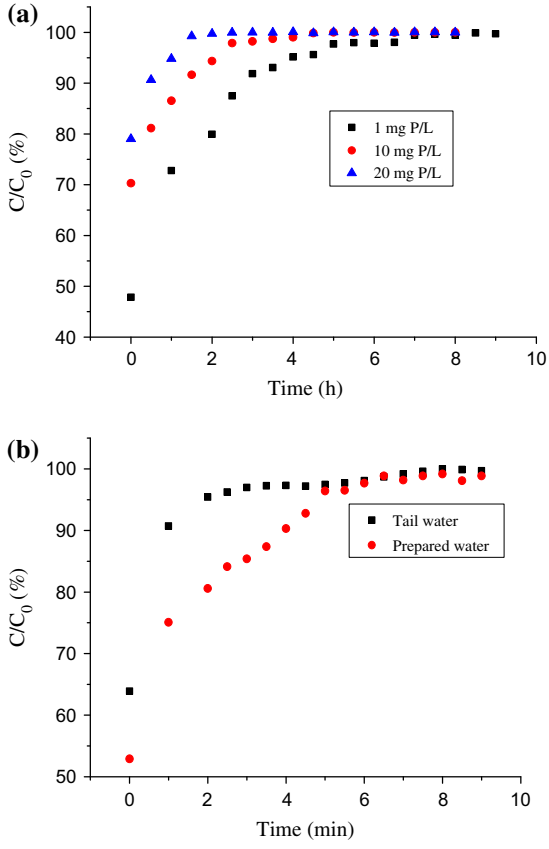

Fig. 6. Effect of (a) concentration, (b) actual tail water on dynamic adsorption of phosphate.

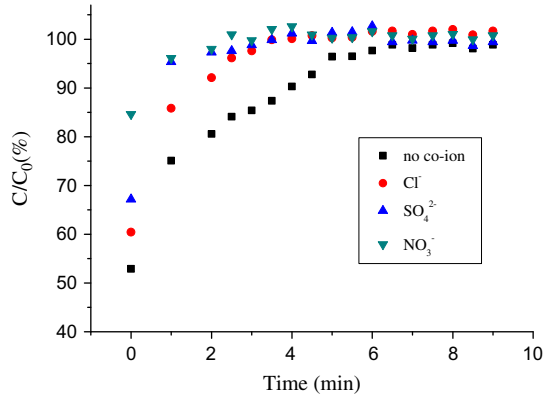

Fig. 7. Effect of interfering ion on dynamic adsorption of phosphate: Cl^-, SO_4^{2-}, NO_3^-.

the P removal amount was 1.44 and 1.46 mg/g, respectively. The limitation of P removal with the increase of $FeCl_3$ percentage demonstrates that the loading of Fe was saturated on GL at high $FeCl_3$ concentration in the impregnation process. This is supported by the fact that about 10% of Fe was determined in the $FeCl_3$ solution after impregnation at the initial $FeCl_3$ percentage of 43%. As a result, the optimal amount of Fe (as Fe_2O_3) loaded on GL was about 0.15 g/g GL, which led to the enhancement of P removal.

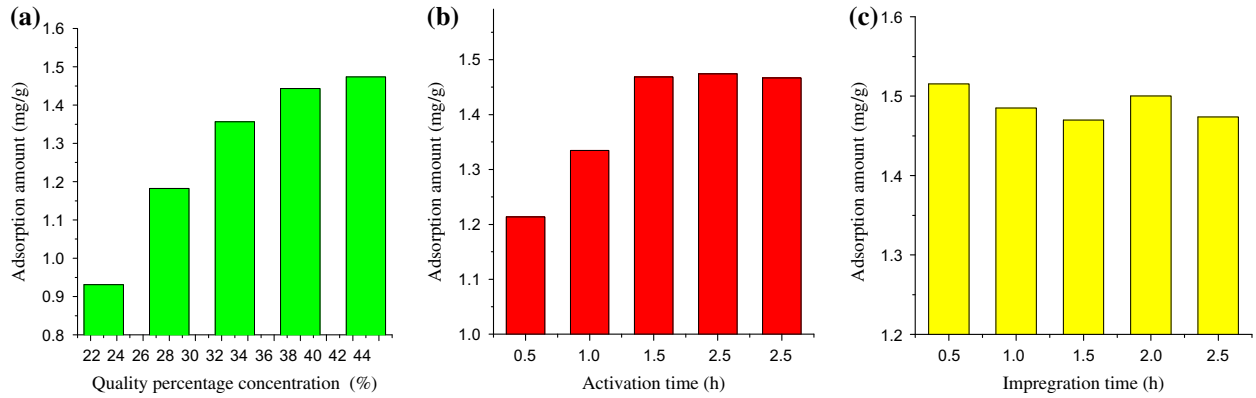

Fig. 8. The effects of different variables on the removal efficiency: (a) activation time (h) = 2, impregnation time (h) = 2.5; (b) $FeCl_3$ solution quality percentage concentration (%) = 43, impregnation time (h) = 2.5; (c) $FeCl_3$ solution quality percentage concentration (%) = 43, activation time (h) = 2.

Table 3
Factors and their levels for central composite design

Variables	Symbol	Coded factor levels		
		−1	0	1
Quality percentage concentration (%)	X_1	23	33	43
Activation time (h)	X_2	0.5	1.5	2.5
Impregnation time (h)	X_3	0.5	1.5	2.5

Table 4
The Box–Behken experimental design and experimental data

Run	Adsorbent preparation variables			
	Quality percentage concentration (x_1)	Activation time (x_2)	Impregnation time (x_3)	Adsorption amount
1	−1	−1	0	0.768
2	1	−1	0	1.216
3	−1	1	0	0.929
4	1	1	0	1.470
5	−1	0	−1	0.957
6	1	0	−1	1.516
7	−1	0	1	0.931
8	1	0	1	1.474
9	0	−1	−1	1.030
10	0	1	−1	1.245
11	0	−1	1	1.002
12	0	1	1	1.211
13	0	0	0	1.207
14	0	0	0	1.207
15	0	0	0	1.207
16	0	0	0	1.206
17	0	0	0	1.194

Fig. 8(b) illustrates the P removal as a function of the activation time. With the time increasing from 0.5 to 1.5 h, the phosphate removal amount increased while kept constant with the time further increasing. This suggests that after 1.5 h, the activated conversion of $FeCl_3$ to Fe_2O_3 was completed as Fe_2O_3 had better affinity toward phosphate.

As shown in Fig. 8(c), the phosphate removal amount was not varied with the increase of impregnation time. This indicates that the Fe could be quickly loaded on, which is contributed to mass transfer or intraparticle diffusion in solid–liquid adsorption process as the adsorption of Fe^{3+} onto GL was controlled by film diffusion [44,45].

3.5.2. Three-dimensional (3D) response surfaces analysis for GL-Fe modification

Based on the single factor experiment in Fig. 8, the relationship between response (phosphate adsorption rate) and three effect factors (quality percentage concentration, activation time, and impregnation time) was analyzed, following the levels of independent factors of the Box–Behken experimental design (Table 3). Accordingly, the adsorption behavior from different batches was evaluated in Design-Expert software by the final estimated response model equation in coded form as follows (Eq. (8)):

$$y = 1.20 + 0.26x_1 + 0.10x_2 - 0.02x_3 + 0.02x_1x_2 - 0.01x_1^2 - 0.10x_2^2 + 0.02x_3^2 \quad (8)$$

where Y is the response denoted as the predicted phosphate adsorption rate, x_1, x_2, and x_3 are the coded terms for three independent variables. As listed in Table 4, a wide range of removal amount of phosphate from a minimum of 0.768 mg/g to a maximum of 1.516 mg/g occurred for the experiment data, indicating that the removal of phosphate was strongly related to the selected variables in the study.

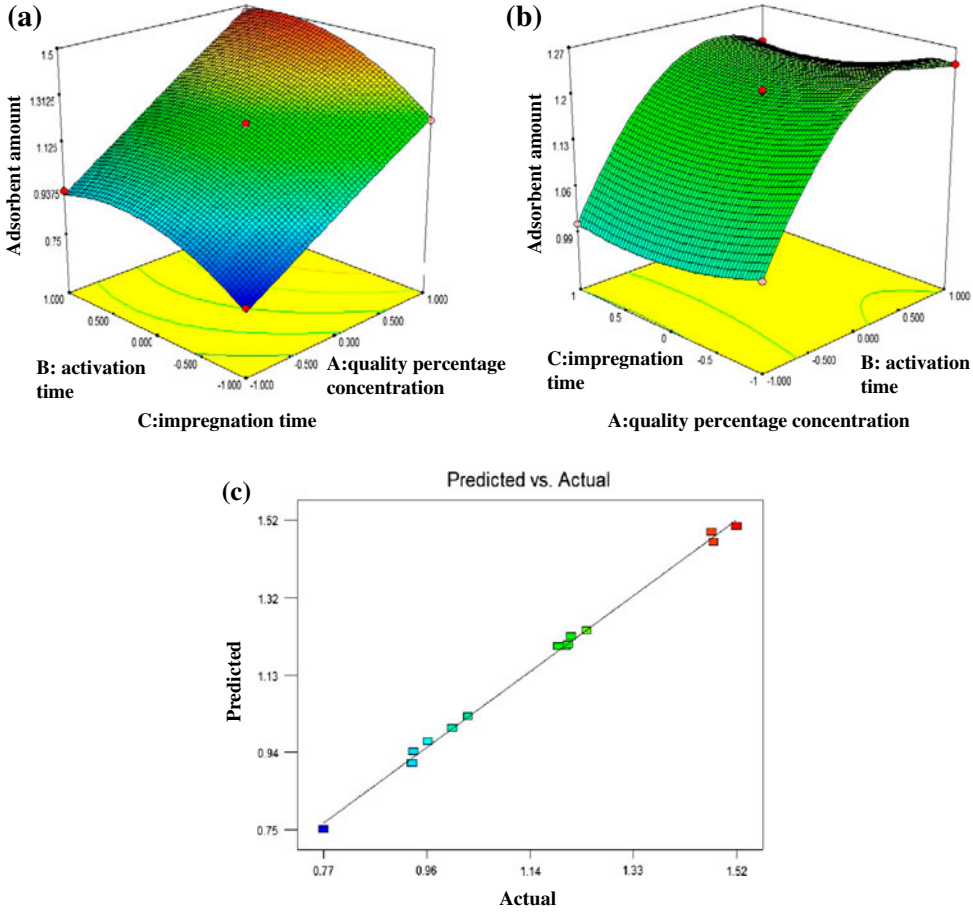

Fig. 9. The 3D response plot of the effects of (a) quality percentage concentration, activation time, and impregnation time = 1.5 h; (b) activation time, impregnation time, and quality percentage concentration = 33%, and (c) the plot of predicted value vs. actual values for removal efficiency.

Moreover, the adequacy of the model was further evaluated by analysis of variance (ANOVA). Fig. 9(a) and (b) illustrates 3D response surfaces analysis result of P removal amount as functions of two variables. There was an interaction effect among the three factors. Fig. 9(c) shows that the predicted vs. actual plots for the removal efficiency where the points were clustered along the diagonal line and the value of R^2 (0.9975) was very close to that of R^2_{adj} (0.9943). This suggests that the predicted values (response) matched well with the observed ones, indicating that the regression model possessed excellent stability. The obtained regression model was adequate to explain most of the variability for phosphate adsorption rate under a given experimental condition. Furthermore, a high degree of precision and reliability of the conducted experiments were confirmed by a low coefficient of variation (C.V. = 0.05%), which was a cue to a goodness fit of the regression model.

Therefore, the optimized conditions of GL-Fe modification were obtained: $FeCl_3$ quality percentage concentration of 43%, activation time of 2.13 h, and impregnation time of 0.5 h. This provided the P adsorption capacity of GL-Fe being 1.542 mg/g in maximum.

4. Conclusions

In this study, GL is prepared by the addition of CMC for the formation of pore structure on GL surfaces. The adsorption of phosphate in batch systems can be described by the Langmuir and Freundlich isotherms, and the adsorption capacity (cal) is 0.572 mg/g. In kinetic experiments, the data in the laboratory and actual phosphorus wastewater were fitted well with the pseudo-second-order model. Batch experiment of P sorption on GL indicates that the pH plays an important role in phosphate sorption. The high phosphate adsorption is achieved in acidic solution. The presence of exogenous competitive ions in solution decreased the phosphate adsorption amount in the order $NO_3^- > SO_4^{2-} > Cl^-$. Moreover, the column adsorption experiments showed that the capacities of the breakthrough and exhaustion points decreased with the increase of the influent concentration and flow rate. This is contributed to the increase of mass transport through the liquid film on the adsorbent surface caused by high influent concentration and flow rate and faster saturation of the bed. On the other hand, a robust and efficient phosphate adsorbent has been developed by loading Fe onto GL. The adequacy of the model based on the RSM design reveals that 1.542 mg/g of P removal amount could be achieved on GL-Fe under the optimum preparation conditions (quality percentage concentration of 43%, activation time of 2.13 h, and impregnation time of 0.5 h, respectively). The results propose that the incorporation method is a highly effective approach to enhance phosphate adsorption performance.

Acknowledgements

The work was supported by National Natural Science Foundation of China (21207085). We also acknowledge support from the Leading Academic Discipline Project of Shanghai Municipal Education Commission (Grant No. S30109).

References

[1] T.S. Anirudhan, B.F. Noeline, D.M. Manohar, Phosphate removal from wastewaters using a weak anion exchanger prepared from a lignocellulosic residue, Environ. Sci. Technol. 40(8) (2006) 2740–2745.
[2] F.W. Gilcreas, Standard methods for the examination of water and waste water, Am. J. Public Health Nations Health 56(3) (1966) 387–388.
[3] L.J. Sherwood, R.G. Qualls, Stability of phosphorus within a wetland soil following ferric chloride treatment to control eutrophication, Environ. Sci. Technol. 35(20) (2001) 4126–4131.
[4] K.S. Narasiah, C. Morasse, J. Lemay, Phosphorus removal from aerated lagoons using alum, ferric chloride and lime, Water Qual. Res. J. Can. 29(1) (1994) 1–18.
[5] D. Mulkerrins, A.D.W. Dobson, E. Colleran, Parameters affecting biological phosphate removal from wastewaters, Environ. Int. 30(2) (2004) 249–259.
[6] J. Paul Chen, M.-L. Chua, B. Zhang, Effects of competitive ions, humic acid, and pH on removal of ammonium and phosphorous from the synthetic industrial effluent by ion exchange resins, Waste Manage. 22(7) (2002) 711–719.
[7] I. de Vicente, P. Huang, F.Ø. Andersen, H.S. Jensen, Phosphate adsorption by fresh and aged aluminum hydroxide. Consequences for lake restoration, Environ. Sci. Technol. 42(17) (2008) 6650–6655.
[8] M.S. Onyango, D. Kuchar, M. Kubota, H. Matsuda, Adsorptive removal of phosphate ions from aqueous solution using synthetic zeolite, Ind. Eng. Chem. Res. 46(3) (2007) 894–900.
[9] E. Galarneau, R. Gehr, Phosphorus removal from wastewaters: Experimental and theoretical support for alternative mechanisms, Water Res. 31(2) (1997) 328–338.
[10] S.J. Shiao, K. Akashi, Phosphate removal from aqueous solution from activated red mud, J. Water Pollut. Control Fed. 49(2) (1977) 280–285.
[11] J. Pradhan, J. Das, S. Das, R.S. Thakur, Adsorption of phosphate from aqueous solution using activated red mud, J. Colloid Interface Sci. 204(1) (1998) 169–172.
[12] E. Oguz, Sorption of phosphate from solid/liquid interface by fly ash, Colloids Surf. A 262(1–3) (2005) 113–117.

[13] N.M. Agyei, C.A. Strydom, J.H. Potgieter, An investigation of phosphate ion adsorption from aqueous solution by fly ash and slag, Cem. Concr. Res. 30(5) (2000) 823–826.
[14] N.M. Agyei, C.A. Strydom, J.H. Potgieter, The removal of phosphate ions from aqueous solution by fly ash, slag, ordinary portland cement and related blends, Cem. Concr. Res. 32(12) (2002) 1889–1897.
[15] V. Cucarella, G. Renman, Phosphorus sorption capacity of filter materials used for on-site wastewater treatment determined in batch experiments–a comparative study, J. Environ. Qual. 38(2) (2009) 381–392.
[16] A. Kaasik, C. Vohla, R. Mõtlep, Ü. Mander, K. Kirsimäe, Hydrated calcareous oil-shale ash as potential filter media for phosphorus removal in constructed wetlands, Water Res. 42(4–5) (2008) 1315–1323.
[17] M. Liira, M. Kõiv, Ü. Mander, R. Mõtlep, C. Vohla, K. Kirsimäe, Active filtration of phosphorus on Ca-rich hydrated oil shale ash: Does longer retention time improve the process? Environ. Sci. Technol. 43 (10) (2009) 3809–3814.
[18] C. Vohla, M. Kõiv, H.J. Bavor, F. Chazarenc, Ü. Mander, Filter materials for phosphorus removal from wastewater in treatment wetlands—A review, Ecol. Eng. 37(1) (2011) 70–89.
[19] A. Tor, N. Danaoglu, G. Arslan, Y. Cengeloglu, Removal of fluoride from water by using granular red mud: Batch and column studies, J. Hazard. Mater. 164 (1) (2009) 271–278.
[20] G. Cappai, G. De Gioannis, A. Muntoni, D. Spiga, J.J.P. Zijlstra, Combined use of a transformed red mud reactive barrier and electrokinetics for remediation of Cr/As contaminated soil, Chemosphere 86(4) (2012) 400–408.
[21] R.C. Sahu, R. Patel, B.C. Ray, Adsorption of Zn(II) on activated red mud: Neutralized by CO_2, Desalination 266(1–3) (2011) 93–97.
[22] E. López, B. Soto, M. Arias, A. Núñez, D. Rubinos, M.T. Barral, Adsorbent properties of red mud and its use for wastewater treatment, Water Res. 32(4) (1998) 1314–1322.
[23] J. Pradhan, S.N. Das, R.S. Thakur, Adsorption of hexavalent chromium from aqueous solution by using activated red mud, J. Colloid Interface Sci. 217(1) (1999) 137–141.
[24] F. Ni, X. Peng, Y. Zhao, J. He, Y. Li, Z. Luan, Preparation of coagulant from red mud and semi-product of polyaluminum chloride for removal of phosphate from water, Desalin. Water Treat. 40(1–3) (2012) 153–158.
[25] W. Huang, S. Wang, Z. Zhu, L. Li, X. Yao, V. Rudolph, F. Haghseresht, Phosphate removal from wastewater using red mud, J. Hazard. Mater. 158(1) (2008) 35–42.
[26] Y. Li, C. Liu, Z. Luan, X. Peng, C. Zhu, Z. Chen, Z. Zhang, J. Fan, Z. Jia, Phosphate removal from aqueous solutions using raw and activated red mud and fly ash, J. Hazard. Mater. 137(1) (2006) 374–383.
[27] H.J. Choi, S.M. Lee, Effect of particle size distribution in wastewater on the performance of nutrient removal process, Desalin. Water Treat. 46(2012) 227–233.
[28] C. Zhu, Z. Luan, Y. Wang, X. Shan, Removal of cadmium from aqueous solutions by adsorption on granular red mud (GRM), Sep. Purif. Technol. 57(1) (2007) 161–169.
[29] J.H. Jang, B.A. Dempsey, Coadsorption of arsenic(III) and arsenic(V) onto hydrous ferric oxide: Effects on abiotic oxidation of arsenic(III), extraction efficiency, and model accuracy, Environ. Sci. Technol. 42(8) (2008) 2893–2898.
[30] K.M. Parida, B. Gorai, N.N. Das, S.B. Rao, Studies on ferric oxide hydroxides, J. Colloid Interface Sci. 185(2) (1997) 355–362.
[31] J.C. Ryden, J.R. McLaughlin, J.K. Syers, Mechanisms of phosphate sorption by soils and hydrous ferric oxide gel, J. Soil Sci. 28(1) (1977) 72–92.
[32] N. Khare, D. Hesterberg, J.D. Martin, XANES investigation of phosphate sorption in single and binary systems of iron and aluminum oxide minerals, Environ. Sci. Technol. 39(7) (2005) 2152–2160.
[33] G. Blanchard, M. Maunaye, G. Martin, Removal of heavy metals from waters by means of natural zeolites, Water Res. 18(12) (1984) 1501–1507.
[34] L. Johansson, Industrial by-products and natural substrata as phosphorus sorbents, Environ. Technol. 20(3) (1999) 309–316.
[35] C.A. Prochaska, A.I. Zouboulis, Removal of phosphates by pilot vertical-flow constructed wetlands using a mixture of sand and dolomite as substrate, Ecol. Eng. 26(3) (2006) 293–303.
[36] C.A. Arias, M. Del Bubba, H. Brix, Phosphorus removal by sands for use as media in subsurface flow constructed reed beds, Water Res. 35(2001) 1159–1168.
[37] M. Kõiv, C. Vohla, R. Mõtlep, M. Liira, K. Kirsimäe, Ü. Mander, The performance of peat-filled subsurface flow filters treating landfill leachate and municipal wastewater, Ecol. Eng. 35(2) (2009) 204–212.
[38] P.W. Schindler, W. Stumm, The surface chemistry of oxides, hydroxides, and oxide minerals, in: W. Stumm (Ed.), Aquatic Surface Chemistry: Chemical Processes at the Particle-Water Interface, John Wiley, New York, NY, 1987, pp. 83–110.
[39] S. Yeoman, T. Stephenson, J.N. Lester, R. Perry, The removal of phosphorus during wastewater treatment: A review, Environ. Pollut. 49(1988) 183–233.
[40] S. Tian, P. Jiang, P. Ning, Y. Su, Enhanced adsorption removal of phosphate from water by mixed lanthanum/aluminum pillared montmorillonite, Chem. Eng. J. 151(1–3) (2009) 141–148.
[41] Q. Zhou, X. Wang, J. Liu, Phosphorus removal from wastewater using nano-particulates of hydrated ferric oxide doped activated carbon fiber prepared by Sol–Gel method, Chem. Eng. J. 200–202 (2012) 619–626.
[42] A. Genz, A. Kornmüller, M. Jekel, Advanced phosphorus removal from membrane filtrates by adsorption on activated aluminium oxide and granulated ferric hydroxide, Water Res. 38(16) (2004) 3523–3530.
[43] L. Rafati, R. Nabizadeh, A.H. Mahvi, M.H. Dehghani, Removal of phosphate from aqueous solutions by iron nano-particle resin Lewatit (FO36), Korean J. Chem. Eng. 29(4) (2012) 473–477.
[44] J. Zhang, Z. Shen, W. Shan, Z. Chen, Z. Mei, Y. Lei, W. Wang, Adsorption behavior of phosphate on Lanthanum(III) doped mesoporous silicates material, J. Environ. Sci. 22(4) (2010) 507–511.
[45] E.I. Unuabonah, K.O. Adebowale, B.I. Olu-Owolabi, Kinetic and thermodynamic studies of the adsorption of lead (II) ions onto phosphate-modified kaolinite clay, J. Hazard. Mater. 144(1–2) (2007) 386–395.